Submitted to The Astrophysical Journal Dec. 8, 2000

Adiabatic Losses and Ultra-High Energy Cosmic Ray Acceleration in Gamma-Ray Burst Blast Waves

Charles D. Dermer[1] and Mayer Humi[2,1]

ABSTRACT

We treat the problem of adiabatic losses and stochastic particle acceleration in gamma-ray burst (GRB) blast waves that decelerate by sweeping up matter from an external medium. The shocked fluid is treated as a homogeneous expanding shell. The energy lost by nonthermal particles through adiabatic expansion is converted to the bulk kinetic energy of the outflow, permitting the evolution of the bulk Lorentz factor Γ of the blast wave to be self-consistently calculated. The behavior of the system is shown to reproduce the hydrodynamic self-similar solutions in the relativistic and nonrelativistic limits, and the formalism is applicable to scenarios that are intermediate between the adiabatic and fully radiative regimes.

Nonthermal particle energization through stochastic gyroresonant acceleration with magnetic turbulence in the blast wave is treated by employing energy-gain rates and diffusive escape timescales based upon expressions derived in the quasilinear regime. This process can accelerate escaping particles to $\gtrsim 10^{20}$ eV energies, consistent with the hypothesis that ultra-high energy cosmic rays (UHECRs) are accelerated by GRB blast waves. Due to particle trapping by the magnetic turbulence, only the highest energy particles can escape during the prompt and afterglow phase of the GRB for acceleration by a Kolmogorov spectrum of MHD turbulence. Lower energy particles begin to escape as the blast wave becomes nonrelativistic and shock Fermi acceleration becomes more important.

Subject headings: cosmic rays—gamma rays: theory—gamma rays: burst

1. Introduction

Cosmic rays are generally believed (Ginzburg and Syrovatskii 1964; Hayakawa 1969) to originate from supernovae (SNe) that accelerate particles in expanding supernova remnants (SNRs). The strongest argument for this belief is that only SNe have the available rates and energies that are required to provide the galaxy-averaged cosmic ray (CR) power of $\approx 5 \times 10^{40}$ ergs s^{-1} (Gaisser 1990) that is inferred by assuming that the locally measured CR spectrum is typical of other locations within the disk of the Milky Way. The particle acceleration mechanism that converts the directed energy of an expanding SNR into nonthermal CRs is widely thought to be first-order Fermi acceleration due to diffusive particle transport across the converging fluid flows in a SNR shock (Drury 1983; Blandford and Eichler 1987). This mechanism is favored because it readily produces a power law with particle number index of -2 in the test particle approximation. This is

[1]E. O. Hulburt Center for Space Research, Code 7653, Naval Research Laboratory, Washington, DC 20375-5352

[2]Mathematical Sciences Department, Worcester Polytechnic Institute, 100 Institute Road, Worcester, MA 01609-2280

close to the value of -2.2 that is required for the CR source injection index, after which particle transport effects steepen the spectrum to an index of -2.75, corresponding to the measured value (e.g., Simpson 1983).

This scenario has not, however, been confirmed. Its most clearcut prediction is the $\pi^0 \to 2\gamma$ feature at 70 MeV due to CR hadronic interactions with gas and dust in the medium surrounding a SNR. A distinct π^0 feature has not been detected in γ-ray spectra of SNRs detected with the EGRET instrument on the *Compton Observatory* (e.g. Esposito et al. 1996), and it is possible to fit the measured spectra with models that employ nonthermal electrons only (Sturner et al. 1997). TeV emission is not detected from SNRs at flux levels expected from secondary hadron production processes (Buckley et al. 1998). In contrast, lepton acceleration by SNRs is implied by X-ray observations of SN 1006 (Koyama et al. 1995), IC 443 (Keohane et al. 1997), and Cas A (Allen et al. 1997), but there is no evidence in these sources for the accelerated CR hadrons that carry the bulk of the local CR power. In addition, the diffuse galactic γ-ray background displays a spectrum that is inconsistent with an origin from CR protons and ions that have the same spectral index as measured locally (Hunter et al. 1997); thus much of the high-energy diffuse emission could be due to radiating leptons (Pohl and Esposito 1998).

The scenario that cosmic rays are accelerated at SNR shocks also meets with significant theoretical problems. Acceleration to energies reaching the knee of the cosmic ray spectrum at $E \simeq 3 \times 10^{15}$ eV has long been known to be difficult to achieve through first order Fermi acceleration, because the timescale for diffusive scattering by turbulence in the ISM limits the maximum particle energy to $E \simeq 10^{14} Z$ eV, where Ze is the ion charge (Lagage and Cesarsky 1983; Baring et al. 1999). The implied composition near the knee of the spectrum is inconsistent with Fermi acceleration by SNRs unless a second component with a carefully adjusted spectrum and composition is assumed (e.g., Protheroe and Szabo 1992). In any case, the SNR hypothesis cannot explain the origin of particles above the knee of the spectrum, for which new Galactic sources are indicated. Finally, the origin of metagalactic ultra-high energy cosmic rays (UHECRs) with $E \gtrsim 10^{19}$ eV remains an unsolved problem that is usually considered separately from the origin of the lower energy CRs (see Nagano and Watson (2000) for a recent review).

Motivated by the coincidence (Waxman 1995; Vietri 1995) between the available power supplied by the sources of GRBs within the Greisen-Zatsepin-Kuzmin radius and the power required to produce the observed energy density of UHECRs, Dermer (2000) recently argued that the high-mass stellar progenitors of GRBs and fireball transients (FTs) are the sources of the hadronic cosmic rays. FTs are probably related to the high-mass ($\gtrsim$ 60-100 $M_\odot$) range of stars that explode as Type Ib/c SNe and collapse to form black holes and eject relativistic flows. They contain as subclasses GRBs and clean and dirty fireballs, the latter two of which have not been detected because of design limitations of currently operating detectors (Dermer et al. 1999). The statistical study of Böttcher and Dermer (2000) shows that the Waxman/Vietri coincidence is maintained under the assumption that the rate density of FTs follows the star formation history of the universe. The power of FTs into the Milky Way is at the level of $\sim 10^{40\pm1}$ ergs s^{-1} (Dermer 2000a). This is marginally adequate to supply power to CR hadrons at the level quoted above, but those estimates may overestimate the required power in view of evidence that CR hadrons have a nonuniform distribution throughout the disk of the Galaxy. Furthermore, the luminosity of the diffuse galactic γ ray emission is $\approx$ 1-3$\times 10^{39}$ ergs s^{-1} (Bloemen et al. 1984) which, if powered primarily by CR leptons, requires considerably less CR power.

In this paper, we consider an alternative scenario for CR origin based upon stochastic particle acceleration and CR production in blast waves that slow from relativistic to nonrelativistic speeds. In Section 2, we consider the adiabatic loss problem in GRB blast waves, and provide an equation for blast-wave evolution that accounts for these losses in a manner that self-consistently rechannels the energy lost from particle expansion into the directed kinetic energy of the expanding blast wave. Stochastic particle acceleration through gyroresonant acceleration is considered in Section 3 by generalizing quasilinear expressions to a fully turbulent regime with relativistic Alfvén speeds, as probably applies to GRB blast waves. We show that UHECR acceleration is possible in relativistic blast waves, and we employ a particle continuity equation to treat particle energy evolution and escape from the blast wave. Simulations of the spectra of particles accelerated in GRB blast waves are presented in Section 4. Particles accelerated through stochastic processes in relativistic blast waves will subsequently participate in shock Fermi processes as the blast wave decelerates to nonrelativistic speeds, so that the difficulty in accelerating cosmic rays to energies past the knee of the CR spectrum may be resolved through this scenario. Summary and conclusions are given in Section 5.

2. Evolution of Blast Wave Lorentz Factor

Both the particles that are captured from an external medium by a GRB blast wave and the ejected thermal plasma particles that initially carry most of the explosion energy will be subject to adiabatic losses due to volume expansion of the blast wave shell. This energy is reconverted into the directed kinetic energy of the outflow. Here we present a treatment of expansion losses in a blast wave that contains particles with arbitrary energies in the comoving frame. The treatment is valid for a blast wave with general values of the bulk speed, and is therefore applicable to both decelerating relativistic GRB blast waves and to nonrelativistic SNR shock waves. The treatment applies to general deceleration regimes from the fully adiabatic to the fully radiative limit.

2.1. Blast-Wave Equation of Motion

Let $p' = \sqrt{\gamma'^2 - 1}$ represent the dimensionless momentum of a particle with Lorentz factor γ', where primes refer to quantities in the comoving frame. The particle distribution function $N'(p'; x)$, integrated over the volume of the blast wave shell, is defined so that $N'(p'; x)dp' = [dN'(p'; x)/dp']dp'$ represents the differential number of particles with momenta between p' and $p' + dp'$ in a blast wave at radius x. In writing this function, we assume that the particles are isotropically distributed in the comoving frame. Global conservation of energy implies that

$$d(\Gamma U_{tot}) = dm + \Gamma dU_{rad} \; . \qquad (1)$$

All masses are in energy units. Here Γ is the Lorentz factor of the blast wave, dm is the differential change in the swept-up rest-mass energy, U_{tot} is the total internal energy in the comoving frame, and dU_{rad} is the differential change in the comoving internal energy that is radiated from the blast wave. The radiated energy is assumed to be isotropically emitted in the comoving frame. We do not take into account energy gains when the system scatters or captures external radiation or magnetic-field energy. Thus equation (1) can apply to internal emission processes such as synchrotron, synchrotron self-Compton, bremsstrahlung, photomeson and secondary nuclear production processes, but not to Compton scattering processes involving external photon fields.

The quantity

$$U_{\rm tot} = \mu m_p \int_0^\infty dp' \gamma' N'(p'; x) \equiv M + U = M_0 + m(x) + U \qquad (2)$$

represents the total internal energy, including rest-mass energy, whereas

$$U = \mu m_p \int_0^\infty dp'(\gamma' - 1)N'(p'; x) \tag{3}$$

represents the internal energy with rest-mass energy excluded. The total rest mass M consists of the sum of the mass $M_0 = E_0/\Gamma_0$ ejected by the explosive event with energy E_0 and initial Lorentz factor Γ_0, in addition to the swept-up mass $m(x) = \int_0^x d\tilde{x}\ [dm(\tilde{x})/d\tilde{x}] = 4\pi\mu m_p \int_0^x d\tilde{x}\tilde{x}^2 n_{ext}(\tilde{x})$. Here $n_{ext}(x)$ is the density of the external medium, and is assumed for simplicity to have radial symmetry. The quantity μ is the ratio of the mass of swept-up particles to the mass of swept-up protons. In most case, the protons make the dominant contribution to the swept-up nonthermal particle energy; thus $\mu = 1$. Generalization to multiple species of swept-up particles, including leptons, ions and charged dust (Schlickeiser and Dermer 2000) is straightforward but is not treated here. The explosion is assumed to be uncollimated, though it is also straightforward to generalize to a system with beamed energy releases and to external media with arbitrary density distributions.

The internal energy U in the blast wave increases by the addition of the kinetic energy of the swept-up matter, and decreases due to particle energy losses through adiabatic expansion and radiation. Thus $dU = dU_m + dU_{adi} + dU_{rad}$, where $dU_m = (\Gamma - 1)dm$ and dU_{adi} represent the changes in internal energy due to swept-up particle kinetic energy and adiabatic losses, respectively. Expanding equation (1) gives $d[\Gamma(U + M)] = \Gamma dU + \Gamma dm + (U + M)d\Gamma$. From this follows the equation of blast wave evolution

$$-\frac{d\Gamma}{\Gamma^2 - 1} = \frac{dm + (\frac{\Gamma}{P^2})dU_{adi}}{M + U}\ , \tag{4}$$

where the blast wave momentum $P = \sqrt{\Gamma^2 - 1}$. Equation (4) can equivalently be written as

$$-\frac{dP}{dx} = \frac{P\Gamma(dm/dx) + (\frac{\Gamma^2}{P})(dU_{adi}/dx)}{M_0 + m(x) + U}\ . \tag{5}$$

The second term in the numerator on the right-hand side of either equation (4) or equation (5) represents the impulse to the blast wave resulting from adiabatic energy losses of the particles in the blast wave. Equation (4) generalizes the equation derived by Panaitescu et al. (1998) for an adiabatic blast wave by the inclusion of radiative losses in the calculation of U and dU_{adi}/dx.

For a strongly radiative blast wave, the adiabatic loss term is small and the radiative equation of blast-wave evolution derived by Blandford and McKee (1976) is recovered by setting $U = dU_{adi}/dx = 0$ and $dm = dM$, giving

$$-\frac{d\Gamma}{\Gamma^2 - 1} = \frac{dm}{M_0 + m(x)} \tag{6}$$

This is easily solved to obtain

$$\Gamma(x) = \frac{[1 + m(x)/M_0]^2(\Gamma_0 + 1) + \Gamma_0 - 1}{[1 + m(x)/M_0]^2(\Gamma_0 + 1) - \Gamma_0 + 1}\ . \tag{7}$$

When radiation losses are included but adiabatic losses are neglected, equation (4) reduces to the form

$$-\frac{d\Gamma}{\Gamma^2 - 1} = \frac{dm}{M_0 + m(x) + U} \tag{8}$$

that is derived from a momentum- and energy-conservation analysis (Dermer and Chiang 1998; Chiang and Dermer 1999; Piran 1999). This equation can be solved (Chiang and Dermer 1999) by noting that

$dU = (\Gamma - 1)dm$. Furthermore, if a fraction ϵ of the swept-up kinetic energy is instantaneously radiated from the blast wave, then $dU = (1-\epsilon)(\Gamma-1)dm$. Defining $\mathcal{M} = M_0 + m(x) + U$ implies that $d\mathcal{M} = [\epsilon + \Gamma(1-\epsilon)]dm$, one obtains

$$- \frac{d\Gamma}{\Gamma^2 - 1} = \frac{d\mathcal{M}}{\mathcal{M}[\epsilon + \Gamma(1-\epsilon)]} \; . \tag{9}$$

Equation (9) has been used to treat partially radiative blast waves (Piran 1999; Böttcher and Dermer 2000; Moderski et al. 2000). Huang, Dai, and Lu (1999, 2000) suggest using the relation $dM = dm[2\Gamma(1-\epsilon)+\epsilon]$ so that the blast-wave evolutionary behavior also follows the Sedov behavior in the adiabatic nonrelativistic regime. Both approaches are adequate to examine the approximate behavior of relativistic blast waves in intermediate radiative regimes, and the treatment of Huang and colleagues furthermore approximates the correct dependence of nonrelativistic adiabatic blast waves. But these approaches do not properly treat adiabatic losses of particles within the blast wave. Moreover, it is necessary to make the assumption that $\epsilon \approx$ const throughout the regime of blast-wave evolution under consideration. When questions of particle acceleration are treated, it is essential to have a correct treatment of adiabatic losses, which equation (5) provides.

2.2. Adiabatic Particle Losses

If the internal energy U in the blast wave is dominated by the kinetic energy of a thermal particle distribution, then U changes due to volume expansion according to the relation $U^{-1}(dU_{adi}/dx) = -(\hat{\gamma} - 1)(d\ln V'/dx)$, where the adiabatic index $\hat{\gamma} = 4/3$ and $5/3$ for relativistic and nonrelativistic monatomic gases, respectively, and V' is the comoving fluid volume. The general case involving a mixed fluid that includes both thermal and nonthermal particles can be derived by noting that p' changes through expansion losses according to the expression

$$- (\frac{dp'}{dx})_{adi} = \frac{p'}{3}\frac{d\ln V'}{dx} \; . \tag{10}$$

Equation (10) reproduces the limiting adiabatic loss forms exhibited by monatomic thermal gases, noting that in the relativistic limit $p' \gg 1$, $d\gamma' \to -(\gamma'/3)d\ln V'$, and in the nonrelativistic limit $p' \ll 1$, $d(p'^2/2) \to -(2/3)(p'^2/2)d\ln V'$.

The comoving volume of the fluid shell is approximated by the expression

$$V' = 4\pi x^2 \Delta' = 4\pi x^2 (\frac{f_\Delta x}{\Gamma}) \; , \tag{11}$$

where Δ' is the comoving width of the blast wave shell. When $f_\Delta = 1/12$, this relation is consistent with the approximation $V' \cong m(x)/(n'm)$ (Panaitescu et al. 1998) in the limits $\Gamma \gg 1$ and $\Gamma - 1 \ll 1$, where $n'(x) = (\hat{\gamma}\Gamma + 1)n_{ext}/(\hat{\gamma} - 1)$ is the downstream comoving density in terms of the external medium density n_{ext}. The differential adiabatic expansion energy-loss rate for particles in a GRB blast wave is therefore given by

$$(\frac{dp'}{dx})_{adi} = -\, p'(\frac{1}{x} - \frac{1}{3}\frac{d\ln\Gamma}{dx}) \; , \tag{12}$$

using equations (10) and (11). Note that the second term on the right-hand-side in the parentheses of equation (12) is small in comparison with the first term in the limit $\Gamma - 1 \ll 1$.

The internal energy therefore changes through adiabatic losses according to the relation

$$\frac{dU_{adi}}{dx} = -\, m_p\, (\frac{1}{x} - \frac{1}{3}\frac{d\ln\Gamma}{dx}) \int_0^\infty dp'\, (\frac{p'^2}{\gamma'})N'(p';x) \; . \tag{13}$$

If only adiabatic losses are important, then equation (12) is easily solved to give

$$p' = p'(x, x_i) = p'_i(\frac{x_i}{x})\,[\frac{\Gamma(x)}{\Gamma(x_i)}]^{1/3}\ , \tag{14}$$

where p'_i is the momentum of a particle injected at radius x_i when the blast wave was moving with Lorentz factor $\Gamma(x_i)$.

The sweep-up function

$$Q_{su}(p'_i, x_i) = \frac{dN'(p'_i, x_i)}{dp'_i dx_i} = 4\pi x_i^2 n_{ext}(x_i)\delta[p'_i - P(x_i)] \tag{15}$$

is defined so that $Q_{su}(p'_i, x_i)dp'_i dx_i$ gives the differential number of particles with comoving-frame momentum p'_i between p'_i and $p'_i+dp'_i$ that are swept-up between radii x_i and x_i+dx_i. The comoving particle distribution function at location x is therefore

$$N'(p'; x) = \int_0^x dx_i |\frac{dp'_i}{dp'}|\ Q_{su}(p', x_i)\ . \tag{16}$$

From the definition of U in equation (3), we obtain

$$U(x) = 4\pi m_p n_0 \int_0^x dx_i x_i^2\ (\bar{\gamma} - 1)\ , \tag{17}$$

where $\bar{p} \equiv (x_i/x)[\Gamma(x)/\Gamma(x_i)]^{1/3}P(x_i)$ and $\bar{\gamma} = \sqrt{\bar{p}^2+1}$. Here the δ-function in equation (15) is used to solve the integral over dp' in equation (3), and we simplify to a uniform surrounding medium with density n_0. Similarly, the dU_{adi}/dx term in equation (13) is evaluated to obtain

$$\frac{dU_{adi}}{dx} = -\ 4\pi m_p n_0\ (\frac{1}{x} - \frac{1}{3}\frac{d\ln\Gamma}{dx})\ \int_0^x dx_i x_i^2\ (\frac{\bar{p}^2}{\bar{\gamma}})\ . \tag{18}$$

Fig. 1 shows a calculation of equation (5) under different assumptions for the particle energy losses. The thermal ejecta particles are assumed to be cold, so that only energy losses of the swept-up particles are considered. The parameters of the calculation are $E_0 = 10^{54}E_{54}$ ergs, $\Gamma_0 = 300\Gamma_{300}$, and $n_0 = 100 n_2$ cm^{-3}, with $E_{54} = \Gamma_{300} = n_2 = 1$. For these parameters, the deceleration radius

$$x_d \equiv (\frac{3E_0}{4\pi\Gamma_0^2 m_p n_0})^{1/3} \cong 2.6\times 10^{16}(\frac{E_{54}}{\Gamma_{300}^2 n_2})^{1/3}\ \mathrm{cm} \tag{19}$$

(Mészáros and Rees 1993). The numerical solution of equation (5), using equations (17) and (18) to calculate the various terms in this equation, is shown by the thick solid curve in the figure. It exhibits the behavior $P(x) \propto x^{-3/2}$ at $x \gg x_d$. This gives the $\Gamma(x) \propto x^{-3/2}$ dependence of Γ at relativistic speeds, and the Sedov solution behavior $\beta(x) \propto x^{-3/2}$ at nonrelativistic speeds, where $P = \beta\Gamma$. For comparison, the dashed lines show the asymptotes for the shocked fluids at relativistic and nonrelativistic bulk Lorentz factors (Blandford and McKee 1976). In the relativistic case, the Lorentz factor of the shocked fluid is given by $\Gamma = (17E/16\pi\rho_0)^{1/2}x^{-3/2}$ when $x \gg x_d$ and $\Gamma \gg 1$, where ρ_0 is the rest-mass energy density of the external medium. In the nonrelativistic case, $\beta \cong 0.29(E/\rho_0)^{1/2}x^{-3/2}$, where we assume that $\hat{\gamma} = 5/3$ is the adiabatic index of the external unshocked gas, and we note that the speed of the shocked fluid is 3/4 of the speed of a nonrelativistic shock.

The analytic solution to the equation of blast-wave evolution in the radiative regime (Blandford and McKee 1976), equation (7), is shown by the labeled solid curve for this case. When $x \gg x_d$, the $P \propto x^{-3}$

behavior is recovered. The analytic solution to the equation for blast-wave evolution with momentum-conservation, equation (9), was derived by Chiang and Dermer (1999) and is shown by the second labeled solid curve in Fig. 1. When $x \gg x_d$, $P \propto x^{-3/2}$ when $P \gg 1$ and $P \propto x^{-3}$ when $P \ll 1$. As pointed out by Huang, Dai, and Lu (1999), this equation does not reproduce the Sedov solution at nonrelativistic Lorentz factors, but rather follows the momentum-conservation equation derived by Oort (Lozinskaya 1992).

2.3. Evolution of Comoving Particle Distribution Function and Internal Energy

When only adiabatic losses are important, the comoving particle distribution function is given by

$$N'(p';x) = 4\pi n_0 \int_0^x dx_i\; x_i^2\; \tilde{D}\; \delta[\tilde{D}p' - P(x_i)] \; , \tag{20}$$

where $\tilde{D} = (x/x_i)[\Gamma(x_i)/\Gamma(x)]^{1/3}$, using equations (14)-(16). The internal energy U_{adi}, for a blast wave subject to adiabatic losses only, is given by substituting equation (20) into equation (3).

The numerical results show that an adiabatic blast wave evolves according to the relation $P(x) \approx P_0$ for $x \ll x_d$, and $P(x) \approx P_0(x/x_d)^{-3/2}$ for $x_d \ll x \ll x_{cool}$, where x_{cool} is the radius when the blast wave becomes strongly radiative (see §2.4). Asymptotes for $N'(p';x)$ and U_{adi} can easily be derived using this expression for $P(x)$. Consider a blast wave that is initially relativistic so that $P_0 \gg 1$. When $x \ll x_d$, $P(x_i) \cong P_0$, $\Gamma(x_i) \cong \Gamma(x) \cong \Gamma_0$, and $\tilde{D} \cong x/x_i$. One obtains

$$N'(p';x) \cong \frac{4\pi n_0}{P_0^3} p'^2\; x^3 H[p' - P_0] \; , \text{ for } x \ll x_d \; , \tag{21}$$

and

$$U_{adi}(x) \cong m_p \pi n_0 x^3 P_0, \text{ for } x \ll x_d \; . \tag{22}$$

The quantity $H[a] = 1$ for $a > 1$ and $H(x) = 0$ otherwise. During the period preceeding deceleration, both the internal energy and total number of particles increases $\propto x^3$, and equation (21) shows that a quadratic tail of particles extending to lower energies is formed due to adiabatic losses.

During the deceleration regime $x_d \ll x \ll \Gamma_0^{2/3} x_d$ while the blast wave is still relativistic, $P(x) \cong \Gamma(x) \cong P_0(x/x_d)^{-3/2}$, and $\tilde{D} = (x/x_i)^{3/2}$. One obtains

$$N'(p';x) \cong \frac{4\pi n_0 x^3}{3} \delta[p' - P_0(\frac{x}{x_d})^{3/2}] \; , \text{ for } x_d \ll x \ll \Gamma_0^{2/3} x_d \; , \tag{23}$$

and

$$U_{adi}(x) \cong \frac{4\pi m_p n_0}{3}\; (x x_d)^{3/2}, \text{ for } x_d \ll x \ll \Gamma_0^{2/3} x_d \; . \tag{24}$$

Equation (23) shows that during this phase, particles maintain a roughly monoenergetic distribution because adiabatic losses of particles balance the slowing down of the blast wave and the energy at which new particles are captured. At the end of the relativistic deceleration phase at $x \cong \Gamma_0^{2/3} x_d$, the internal energy $U_{adi} \cong E_0$, that is, a large fraction of the fireball kinetic energy has been transformed into internal particle energy within the shell.

The decelerating blast wave becomes nonrelativistic when $x \gg \Gamma_0^{2/3} x_d$. In this regime, $P(x) \cong P_0(x/x_d)^{-3/2}$, $\Gamma(x) \cong \Gamma(x_i) \cong 1$, and $\tilde{D} \cong x/x_i$. The comoving distribution function and internal energy of particles that are swept in *after* the blast wave becomes nonrelativistic are

$$N'(p';x) \cong 8\pi n_0\; \frac{P_0^6 x_d^9}{p'^7 x^6}\; H[p; P_0(\frac{x}{x_d})^{-3/2}, P_0^{2/3}(\frac{x_d}{x})], \text{ for } x \gtrsim \Gamma_0^{2/3} x_d \; , \tag{25}$$

and

$$U_{adi}(x) \cong \pi m_p n_0\; P_0^2 x_d^3 [1 - P_0^{4/3} (\frac{x_d}{x})^2],\ \text{for}\ x \gtrsim \Gamma_0^{2/3} x_d\ , \tag{26}$$

respectively. In equation (23), $H[y;a,b] = 1$ for $a \le y < b$ and $H[y;a,b] = 0$ otherwise. Comparing equations (24) and (26), one sees that the internal energy approaches a constant value.

The inset in Fig. 1 shows the numerical calculation of the internal energy U_{adi}. The above asymptotes can be seen to agree with these calculations. The difference between the adiabatic and momentum-conservation solutions can be appreciated by noting that in the absence of adiabatic losses,

$$U_{mom}(x) = 4\pi m_p n_0 \int_0^x dx_i x_i^2\; [\Gamma(x_i) - 1]\ . \tag{27}$$

Because particles experience no adiabatic losses in the momentum-conservation solution, the internal energy will always be greater than in the adiabatic case where such losses are included. Using equation (27), one sees that $U_{mom} \cong (4/3) U_{adi}$ when $x \ll x_d$, and $U_{mom} \cong 2U_{adi}$ when $x \gg x_d$ noting that very little additional internal energy is swept into the blast wave when $x \gtrsim \Gamma_0^{2/3} x_d$. During the episode of deceleration while the blast wave is relativistic, most of the internal energy is swept-up when $x \cong x_i$, so that $\bar{p}(x_i) \cong P(x)$ and $\bar{\gamma} \cong \Gamma(x)$ in equation (17). Thus the relativistic forms of the adiabatic and momentum-conservation solutions are similar. Most of the internal energy that remains within the blast wave as it decelerates to nonrelativistic speeds was introduced during the relativistic phase. The greater amount of internal energy for the momentum-conservation solution means that the blast wave must travel more slowly than in the adiabatic solution in order to conserve total momentum.

The dependences in the various limits are obtained by noting that for the momentum-conservation solution, $P\{M_0 + \int_0^x d\tilde{x}[dm(\tilde{x})/d\tilde{x}]\Gamma(\tilde{x})\} \cong \beta\Gamma[M_0 + m(x)\Gamma(x)] \cong \beta\Gamma[M_0 + kx^3\Gamma] \cong$ const, giving the asymptotes $\Gamma \propto x^{-3/2}$ when $\Gamma_0 \gg \Gamma \gg 1$ and $\beta \propto x^{-3}$ when $\Gamma - 1 \ll 1$. For the radiative solution, $P\{M_0 + \int_0^x d\tilde{x}[dm(\tilde{x})/d\tilde{x}]\} \cong \beta\Gamma[M_0 + m(x)] \cong \beta\Gamma[M_0 + kx^3] \cong$ const, giving the asymptotes $\Gamma \propto x^{-3}$ when $\Gamma_0 \gg \Gamma \gg 1$ and $\beta \propto x^{-3}$ when $\Gamma - 1 \ll 1$. The limits for the adiabatic solution would seem to be obtained through total energy conservation from the expression $\Gamma\{M_0 + \int_0^x d\tilde{x}\Gamma(\tilde{x})[dm(\tilde{x})/d\tilde{x}]\} \cong \Gamma[M_0 + \Gamma m(x)] \cong \Gamma[M_0 + kx^3(\Gamma - 1)] \cong$ const. This gives the correct relativistic asymptote $\Gamma \propto x^{-3/2}$ when $\Gamma_0 \gg \Gamma \gg 1$, but implies that $\beta \propto x^{-3}$ when $\Gamma - 1 \ll 1$. As is apparent from the numerical results, the change in internal energy due to adiabatic losses becomes important in the nonrelativistic regime so that this estimate is not valid there.

2.4. Nonrelativistic Limit of Equation for Blast-Wave Evolution

The evolution of the speed of a nonrelativistic blast wave is described by the equation

$$-\frac{d(M\beta)}{dt} = \frac{1}{\beta}\,\frac{dU_{adi}}{dt} + U\frac{d\beta}{dt}\ , \tag{28}$$

which is obtained by letting $P \to \beta$, $\Gamma \to 1$, and $dx \to \beta c dt$ in equation (5). Because $dU_{adi}/dt \simeq (\beta c)^{-1} U/x$ and $\beta \ll 1$, this term dominates the $U d\beta/dt$ term in equation (28). When consideration of the external medium pressure on blast-wave evolution is taken into account, we recover the equation of Cowsik and Wilson (1975). This was used to establish the important result that if SNe are the sources of cosmic rays below the knee of the CR spectrum, then CR acceleration must persist during the late phases of SNR evolution in order to overcome adiabatic energy losses within the expanding remnant.

The dotted curve in Fig. 1 shows the dependence

$$P(x) = \frac{P_0}{\sqrt{1+(x/x_d)^3}} \cong \begin{cases} P_0\ , & \text{for } x \ll x_d \\ \beta_0(\frac{x}{\ell_S})^{-3/2}\ , & \text{for } x_d \ll x \ll x_{cool} \end{cases} \tag{29}$$

suggested by the solution (Chiang and Dermer 1999) to the equation for momentum conservation. This provides a representation that is accurate to within 10% of the numerical solution and the hydrodynamical asymptotes describing the behavior of an adiabatic blast wave. The Sedov length

$$\ell_S \equiv \Gamma_0^{2/3} x_d = (\frac{3E_0}{4\pi\mu n_0 m_p})^{1/3} \cong 5.4\times 10^{18}\,(\frac{E_{54}}{n_0})^{1/3}\ \text{cm} = 1.76(\frac{E_{54}}{n_0})^{1/3}\ \text{pc} \tag{30}$$

(Sari et al. 1996).

At nonrelativistic energies, $(M_0 + 4\pi x^3 n_0 \mu m_p/3)v = M_0 v_0$ from momentum conservation, where $v = v(x)$ and v_0 is the initial speed of the ejecta. Thus the SN ejecta begin to undergo significant deceleration when the swept-up mass is about equal to the ejecta mass, that is, when $x = \ell_S$. When $\Gamma_0 - 1 \ll 1$, $x_d \approx \ell_S$, recalling that $E_0 \to M_0$ in this limit.

In the nonrelativistic limit with $P_0 \ll 1$, equation (29) reduces to

$$P(x) \to \beta(x) \cong \begin{cases} \beta_0 = v_0/c\ , & \text{for } x \ll x_d \cong \ell_S \\ \beta_0(\frac{x}{\ell_S})^{-3/2} = (\frac{3E_{ke}}{2\pi\rho_0})^{1/2} x^{-3/2}\ , & \text{for } \ell_S \ll x \ll x_{cool} \end{cases}\ . \tag{31}$$

where $E_{ke} \equiv \beta_0^2 E_0/2$ is the kinetic energy of the injection event when $\beta_0 \ll 1$, and $\rho_0 \equiv m n_0$ is the rest-mass energy density of the CBM. From the nonrelativistic branch in equation (31), we see that

$$\beta(x) = 0.10(\frac{E_{51}}{n_0})^{1/2}\,[x(\text{pc})]^{-3/2}\ , \tag{32}$$

where E_{51} is the explosion kinetic energy in units of 10^{51} ergs. For comparison, Lozinskaya (1992) gives the relation $\beta(x) = [4\times 2.02 \times E_{ke}/(25\times\rho_0)]^{1/2} x^{-3/2} = 0.086(E_{51}/n_0)^{1/2}[x(\text{pc})]^{-3/2}$, obtained from the hydrodynamic self-similar Sedov solution. When $x \gg x_{cool}$, the Sedov phase ends. Chevalier (1974) and Falle (1981) find that due to the onset of atomic and bremsstrahlung processes in the cooling plasma, $x_{cool}(\text{pc}) = 19E_{51}^{0.29}n_0^{-0.41}$ and $x_{cool}(\text{pc}) = 20E_{51}^{0.295}n_0^{-0.409}$, respectively (see also Lozinskaya (1992)).

3. Particle Acceleration in GRB Blast Waves

Particle acceleration can occur in GRB blast waves through a first-order Fermi mechanism involving internal or external shocks, and through second-order Fermi acceleration involving gyroresonant scattering of particles by magnetic turbulence in the magnetic field of the blast wave. Waxman (1995) and Waxman and Bahcall (2000) argue that shocks within a relativistic wind that persists over a timescale characteristic of the duration of a GRB could accelerate particles to UHECR energies. Such a blast wave must be highly radiative in order to give good efficiency for UHECR production; otherwise the bulk of the energy of the explosion is retained within the blast wave to be radiated during the afterglow phase when acceleration ceases and adiabatic losses reduce the energy of the nonthermal particles. UHECR acceleration in an internal shock model must also compete with strong photomeson losses that could limit acceleration to the highest energies.

An external shock acceleration model for UHECR acceleration has been shown to be infeasible (Gallant and Achterberg 1999). Following the first shock crossing, subsequent energy gains are modest because cosmic rays that diffuse in the surrounding medium are captured before pitch angle scattering changes the direction of the CR with respect to the shock normal by more than $\sim 1/\Gamma$.

We therefore consider stochastic acceleration within the GRB blast wave. Wave turbulence in the magnetic field of the blast wave will be generated through the process of capturing electrons, protons, and charged dust (Pohl and Schlickeiser 2000; Schlickeiser and Dermer 2000). Rayleigh-Taylor instabilities in the expanding fluid and density irregularities in the surrounding medium will also introduce magnetohydrodynamic turbulence on sizes corresponding to the blast-wave width. This energy will cascade to MHD turbulence on smaller size scales. Although the wave generation and cascading process is inherently dynamic, we approximate the turbulence spectrum by a power-law in wavenumber space in order to provide a simplified treatment of the process.

3.1. Maximum Energy of Particles Retained in GRB Blast Waves

Allowed sites of UHECR acceleration must satisfy the Hillas (1984) condition, which essentially requires that the particle Larmor radius $r_{\rm L}$ be less than the size scale D of the system. For GRB blast waves, $r_{\rm L} = (m_p/eB)p'(A/Z)$, where B is the mean magnetic field, Am_p is the ionic mass and Ze its charge, and $D = \Delta'$. When generalized for bulk relativistic motion of the acceleration region (e.g., Waxman (1995); Norman et al. (1995)), the maximum measured particle energy that can be accelerated in a GRB blast wave is $E_{max}({\rm ergs}) = \Gamma e Z B \Delta'$.

The value of B is conventionally assigned in terms of a magnetic field parameter e_B that gives the magnetic field energy density in terms of the energy density of the downstream shocked fluid. Thus

$$B = (32\pi\mu n_0 e_B m_p)^{1/2}\sqrt{\Gamma(\Gamma-1)} = 0.39(e_B\mu n_0)^{1/2}P\sqrt{\Gamma/(1+\Gamma)}\ {\rm Gauss} \cong 0.39(e_B\mu n_0)^{1/2}P\ {\rm Gauss}\ , \quad (33)$$

where the approximation is valid to within a factor of $\sqrt{2}$ from the extreme relativistic to the nonrelativistic regime. Recalling the definitions of Δ' in equation (11) and x_d from equation (19), we therefore see that $p \cong \Gamma p' < 0.39e(e_B\mu n_0)^{1/2} Z f_\Delta x\sqrt{\Gamma(\Gamma-1)}/Am_p$, implying

$$E_{max}({\rm eV}) \cong 7.6\times 10^{20} Z(\frac{f_\Delta}{1/12})(\mu n_2)^{1/6} e_B^{1/2}(E_{54}\Gamma_{300})^{1/3}(\frac{\Gamma}{\Gamma_0})(\frac{x}{x_d})\sqrt{1-\Gamma^{-1}}\ . \quad (34)$$

The value of E_{max} depends on x and P, but we can see that at the deceleration timescale

$$t_d \equiv \frac{x_d}{P_0\Gamma_0 c}\ , \quad (35)$$

where $\Gamma \cong \Gamma_0$ and $x \cong x_d$, energetic GRBs can in principle accelerate protons and ions to $\gg 10^{20}$ eV.

The Hillas condition when applied to electrons with $Z = 1$ also yields equation (34). Once ions begin escaping from the acceleration region, however, electrostatic forces may develop to modify the lepton escape rate. Moreover, synchrotron radiation losses are much more important for leptons, as we see quantitatively in Section 3.2.6, and these losses will impede lepton acceleration to energies set by this condition.

The relationship between x and observer time $t \equiv t_d\tau$ is obtained by noting that $dx \cong P\Gamma c dt$. Assuming an adiabatic blast wave, we can use equation (29) to obtain

$$\frac{x}{x_d} \cong \begin{cases} \tau\ , & \text{for } \tau \ll 1 \\ (4\tau)^{1/4}\ , & \text{for } 1 \ll \tau \ll \Gamma_0^{8/3} \\ (5\tau/2\Gamma_0)^{2/5}\ , & \text{for } \tau \gg \Gamma_0^{8/3}, \end{cases} \quad (36)$$

from which it follows that

$$\frac{P}{P_0} \cong \begin{cases} 1\,, & \text{for } \tau \ll 1 \\ (4\tau)^{-3/8}\,, & \text{for } 1 \ll \tau \ll \Gamma_0^{8/3} \\ (5\tau/2\Gamma_0)^{-3/5}\,, & \text{for } \tau \gg \Gamma_0^{8/3} \end{cases} \tag{37}$$

and

$$\frac{\Gamma}{\Gamma_0} \cong \begin{cases} 1\,, & \text{for } \tau \ll 1 \\ (4\tau)^{-3/8}\,, & \text{for } 1 \ll \tau \ll \Gamma_0^{8/3} \\ \Gamma_0^{-1}[1+\frac{P_0^2}{2}\,(\frac{5\tau}{2\Gamma_0})^{-6/5}]\,, & \text{for } \tau \gg \Gamma_0^{8/3}. \end{cases} \tag{38}$$

Expressions (36)-(38) apply to initially relativistic or nonrelativistic blast waves, but in the latter case the middle branches do not obtain insofar as $\Gamma_0 \approx 1$. The late-time ($\tau \gg \gamma_0^{8/3}$) behavior of the nonrelativistic expressions persists until the blast wave becomes highly radiative. In the nonrelativistic regime, the blast wave radius depends upon observer time according to the relation $x = (75\beta_0^2 E_0 c^2/16\pi n_0 m_p)^{1/5} t^{2/5} = 0.36(E_{51}/n_0)^{0.2} t^{0.4}(\text{yr})$ pc, in good agreement with the Sedov-Taylor self-similar solution (Lozinskaya 1992).

Equations (34-38) show that UHECR production in GRB blast waves is in accord with the Hillas limit throughout the prompt and afterglow phase of a GRB for suitably energetic GRBs when $e_B \sim 1$. The $\sim \tau^{-1/8}$ dependence during the afterglow phase implies a reduction in E_{max} by about one order of magnitude during the relativistic phase of a GRB blast wave, assuming that all other parameters remain constant. During the nonrelativistic phase, this dependence steepens to $E_{max} \propto \tau^{-1/5}$. Insofar as the bulk of the total energy liberated by fireball transients and GRBs is emitted by the relatively infrequent, very energetic explosions with $E_{54} \gg 0.1$ (Dermer 2000), and that GRBs probably occur in very dense star forming regions (van Paradijs et al. 2000; Dermer and Böttcher 2000), GRB blast waves satisfy the Hillas condition and are viable acceleration sites for UHECR production.

3.2. Stochastic Particle Acceleration

Our treatment of stochastic gyroresonant particle acceleration is very simplified. We make use of systematic energy gain rates and diffusive escape timescales based upon expressions derived in the quasilinear regime (Melrose 1974; Miller and Ramaty 1989; Bogdan et al. 1991), and consider only parallel-propagating modes that resonate with particles through the Doppler or anomalous Doppler resonance. The most important modes for protons and ions are shear Alfvén waves, including ion-cyclotron waves, whereas electrons will gyroresonate with fast mode waves, including whistlers. We assume that the spectrum of parallel waves can be described by the function $w(k) \propto k^{-q}$, where $w(k)dk$ is the differential energy density in waves with wave numbers between k and $k + dk$ and q is the spectral index of the turbulence. For a Kolmogorov spectrum of turbulence, $q = 5/3$. Assuming symmetry between the direction of wave propagation so that $w(k) = w(-k)$, the ratio of energy density in waves to the magnetic-field energy density $u_B = B^2/8\pi$ is given by $\zeta \equiv 2\int_{k_min}^{\infty} dk\; w(k)/u_B$. The smallest wave number k_{min} is related to the largest size scale on which turbulence is generated. For a blast wave, we therefore assign $k_{min} \approx 1/\Delta'$.

In the quasilinear regime, the systematic energy-gain rate for stochastic particle acceleration implied by the pitch-angle-averaged momentum diffusion coefficient with shear Alfvén turbulence is given by

$$\langle\frac{d\gamma'}{dt}\rangle_{sto} = \frac{\pi}{2}(\frac{q-1}{q})\beta_A^2\zeta(ck_{min})(r_L^0 k_{min})^{q-2}p'^{q-1} \tag{39}$$

(Melrose 1974; Miller and Roberts 1995; Dermer et al. 1996), where $c\beta_A = B/\sqrt{4\pi n' m_p}$ is the Alfvén speed and $r_L^0 \equiv (m_p/eB)(A/Z)$ is the nonrelativistic Larmor radius of the particle, so that $r_{\rm L} = r_{\rm L}^0 p'$. Expression

(39) also holds for gyroresonance with fast-mode waves away from the whistler branch. The magnetic-field prescription (33) implies that $\beta_{\rm A} \simeq 2^{3/2} e_B^{1/2} P$. In order to accelerate UHECRs in GRB blast waves [eq.(34)], we require that $e_B \approx 1$, implying that $\beta_A \gg 1$. We interpret this unphysical result to indicate that the Alfvén velocity approaches c whenever $P \gtrsim 1$ and $e_B \sim 1$. We also assume that $\zeta \gtrsim 0.1$, so that the magnetic field approaches the fully turbulent regime. When these conditions hold, stochastic particle acceleration is very rapid because the scattering centers are traveling at speeds approaching c, and the scattering rate is large. This is contrary to the usual situation found in the interstellar medium, where $\beta_A \sim 10^{-4}$ and ζ may be $\ll 1$.

These conditions violate, however, the quasilinear assumptions used to derive the stochastic transport coefficients leading to equation (39). We nevertheless assume that this expression still provides the correct functional dependence on p' and q, so that

$$\dot{p}'_{sto} = K_p (c/\Delta')(r_L^0/\Delta')^{q-2} p'^{q-1} \;, \tag{40}$$

where $K_p \lesssim 1$. Consequently

$$(\frac{dp'}{dx})_{sto} = \frac{\dot{p}'_{sto}}{Pc} = \frac{K_p}{P r_L^0}\,(\frac{r_L^0 p'}{\Delta'})^{q-1} \;. \tag{41}$$

Particles will diffuse via pitch-angle scattering and subsequently escape from the blast-wave shell. The diffusive escape timescale along the direction of the large scale magnetic field is given in the quasilinear regime by

$$t'_{esc} \approx \max[t'_{dyn}, \frac{\pi}{8}(q-1)(2-q)(4-q) t'_{dyn} \zeta (r_L^0 k_{min})^{q-2} p'^{q-2}] \tag{42}$$

(Barbosa 1979; Steinacker and Miller 1992; Schlickeiser 1989; Dermer et al. 1996), where $t'_{dyn} \approx \Delta'/c$ represents the transit timescale for straight-line escape from the blast wave. Because much of the application in this paper falls outside the quasilinear regime, we again assume that the quasilinear proportionality holds and write

$$t'_{esc} \approx t'_{dyn} \max[1, K_t (\frac{r_L^0 p'}{\Delta'})^{q-2}] \;. \tag{43}$$

The values that K_t can assume are poorly known because K_t depends on the magnetic field direction in the blast wave. If the magnetic field is primarily radial, then K_t could be $\ll 1$. If there is a significant transverse magnetic field, then diffusive escape from the blast wave will be inhibited so that $K_t \gg 1$.

3.2.1. Comparison between Available Time and Stochastic Gain Rates

The highest energy a particle can reach is limited by the time available for particle acceleration. This maximum energy can be determined by solving the equation $dp'/dx = (dp'/dx)_{sto}$, using equation (41). Considering only proton ($A/Z = 1$) acceleration in the relativistic regime $\Gamma \gg 1$, we find that

$$p'^{2-q}_{max,av} \cong p'^{2-q}_i + \frac{K_p (9.6 \times 10^7)^{q-1} (e_B \mu n_0)^{(2-q)/2}}{8.0 \times 10^6}\,(x^{2-q} - x_i^{2-q}) \;, \tag{44}$$

where p'_i and x_i refer to the injection momenta and location. For a Kolmogorov spectrum with $q = 5/3$, $p'_{max,av} \cong 1.8 \times 10^{-4} K_p^3 \sqrt{e_B \mu n_0} x$. For standard parameters with $x_d = 2.6 \times 10^{16}$ cm and $\Gamma_0 = 300$, $p_{max,av} \cong \Gamma p'_{max,av} \cong 1.4 \times 10^{15} K_p^3 \sqrt{e_B}$ at $x = x_d$. Thus the available time constraint does not prevent acceleration to ultra-high energies unless $K_p \ll 1$.

3.2.2. Comparison between Adiabatic Loss and Stochastic Gain Rates

Particles will be stochastically accelerated to higher energies until adiabatic losses prevent further acceleration. This energy is given by the condition $(dp'/dx)_{sto} < |(dp'/dx)_{adi}| \cong p'/x$, where the last expression follows from equation (10), noting that $|(dp'/dx)_{adi}| = (1 + g/3)/x$ for $\Gamma(x) \propto x^{-g}$. Even for a radiative blast wave with $g = 3$, the expression $-p'/x$ for the adiabatic energy-loss rate is valid to within a factor of 2. This relation also roughly compares the timescale for a particle to be accelerated to some value of p' against the available time. One finds that the maximum momentum until adiabatic losses dominates is given by

$$p_{max,adi} = \Gamma p'_{max,adi} = (12K_p)^{1/(2-q)}\,(\frac{\Gamma\Delta'}{r^0_{\rm L}})\ . \tag{45}$$

Recalling the Hillas condition $p < \Gamma\Delta'/r^0_{\rm L}$, we therefore see that the maximum energy that a particle can attain, subject to adiabatic losses, is

$$E_{max,adi} = (12K_p)^{1/(2-q)}E_{max}\ , \tag{46}$$

where we have set $f_\Delta = 1/12$. Thus we see that particles can be accelerated to energies given by equation (34) if $K_p \gtrsim 1/12$. It is also interesting to note that if $q = 2$, adiabatic losses will never dominate stochastic particle acceleration when $K_p \gtrsim 1/12$, and will always dominate acceleration if $K_p \lesssim 1/12$.

3.2.3. Comparison between Diffusive Escape and Comoving Timescales

When the timescale for a particle with a given momentum to escape diffusively from the blast wave is shorter than the comoving timescale, then acceleration to larger momenta is no longer possible. This condition is $K_t(\Delta'/c)(r^0_L p'/\Delta')^{q-2} < t' \cong x/(cP)$, implying that $p_{max,esc} = (\Gamma\Delta'/r^0_{\rm L})(K_t f_\Delta)^{1/(2-q)}$. Consequently

$$E_{max,esc} \geq (K_t/12)^{1/(2-q)}E_{max}\ . \tag{47}$$

The inequality applies when the transit timescale exceeds the diffusive escape timescale (eq. [43]). Equation (47) shows that if $K_t \gtrsim f_\Delta^{-1} \cong 12$, as could occur for large transverse magnetic fields in the blast wave, then particles will not diffuse from the blast wave during the available time before being accelerated to energies limited by the Hillas condition.

3.2.4. Comparison between Stochastic Energy Gain and Diffusive Escape Timescales

Acceleration to a given energy will be limited by the diffusive escape from the blast wave. The inverse of the timescale for stochastic acceleration is $t^{-1}_{sto} = K_p(c/\Delta')(r^0_{\rm L}p'/\Delta')^{q-2}$. Comparing with the diffusive escape timescale (43) gives $p < (\Gamma\Delta'/r^0_{\rm L})(K_pK_t)^{1/(4-2q)}$, or

$$E_{max,acc/esc} = (K_pK_t)^{1/(4-2q)}E_{max}\ . \tag{48}$$

Thus we see that particles can be accelerated through stochastic gyroresonance to ultra-high energies if $K_pK_t \gtrsim 1$, limited only by the condition that the Larmor radius is smaller than the blast wave width, if $K_p \gtrsim f_\Delta$ and $K_t \gtrsim 1/f_\Delta$. When $q = 2$, particles can either be accelerated to arbitrarily high energies if $K_pK_t \gtrsim 1$, or will not be accelerated if $K_pK_t \lesssim 1$.

3.2.5. Comparison between Stochastic Energy Gain and Synchrotron Radiation Losses

The synchrotron loss rate for particles with randomly oriented pitch angles in a magnetic field with mean strength B is given by $-\dot{\gamma}'_{syn} = 4c\sigma_{\rm T}Z^4(B^2/8\pi)p'^2/[3A^3(m_p/m_e)^3]$. Hence

$$-\dot{\gamma}'_{syn} = \frac{16}{3}\,\frac{\mu Z^4}{A^3}\,\frac{c\sigma_{\rm T}e_B n_0\Gamma(\Gamma-1)}{(m_p/m_e)^2}\,p'^2 \cong -\dot{p}'_{syn} \tag{49}$$

Equating this rate to the stochastic energy gain rate (40) gives the maximum particle momentum achievable due to the competition with synchrotron losses. The result is

$$p_{max,syn} \cong \Gamma[\frac{K_p}{\Delta'}\,(\frac{r_{\rm L}^0}{\Delta'})^{q-2}\,\frac{3A^3}{16\mu Z^4}\,\frac{(m_p/m_e)^2}{\sigma_{\rm T}e_B n_0\Gamma(\Gamma-1)}]^{1/(3-q)}\ . \tag{50}$$

Figs. 2a-d show calculations of E_{max} for protons implied by the Hillas condition, equation (34), compared with the maximum energy $E_{max,syn}({\rm eV}) \cong 9.4\times 10^8 A p_{max,syn}$ determined by comparing the stochastic particle acceleration energy-gain rate with the synchrotron energy-loss rate from equation (50). Hence $A = 1$, $Z = 1$, and we let $\mu = 1$. The standard parameter set employs a Kolmogorov turbulence spectrum with $q = 5/3$, $e_B = \Gamma_{300} = n_2 = E_{54} = K_p = 1$, and $f_\Delta = 1/12$. The lower set of curves in each figure gives the Hillas condition result, and these curves are independent of the level of turbulence and particle acceleration rate set by K_p. The limits set by available time, adiabatic losses, diffusive escape, and the particle acceleration rate give maximum energies proportional to E_{max}, as seen in Sections 3.2.1 - 3.2.4. The upper set of curves gives the maximum energy $E_{max,syn}$ determined by the competition between particle acceleration and synchrotron losses. When these latter curves are less than E_{max}, then the maximum possible particle energy is set by $E_{max,syn}$.

For the standard parameter set, $x_d = 2.6\times 10^{16}$ cm and $\ell_{\rm S} = \Gamma_0^{2/3}x_d \cong 10^{18}$ cm. The dissipation of directed kinetic outflow into internal particle energy is greatest for an adiabatic blast wave over this range of distances. Thus if GRBs are the sources of UHECRs, then the values of E_{max} reached between x_d and $\ell_{\rm S}$ determine whether GRBs are viable sites of UHECRs. As can be seen, there are wide ranges of parameter values that permit particle acceleration to proton energies $\gtrsim 10^{20}$ eV. Because more energetic ions can have comparable Larmor radii than less energetic protons due to their larger charges, ions can reach even larger energies than protons subject to the Hillas condition. Synchrotron losses can, however, restrict the maximum particle energy to smaller values for ions than for protons. Other radiative losses, in particular, photomeson production of high energy particles interacting with synchrotron photons radiated by relativistic electrons in a GRB blast wave, can also prevent particle acceleration to ultra-high energies. This process has been treated by Dermer (2000) in detail for an external shock model, and is shown not to limit ultra-high energy particle acceleration.

Figs. 2a-2c show that E_{max} generally increases for increasing values of Γ_0, E_{54}, and n_2, with all other parameters remaining constant. For the largest values of E_{54} and n_2 that are considered, synchrotron losses rather than the Hillas condition determine the maximum particle energies. Fig. 2d illustrates the effects of changing K_p, q, and e_B on E_{max}. Changing K_p and q has no effect on E_{max} but does change $E_{max,syn}$. If $K_p \lesssim 0.1$, UHECR particle acceleration becomes infeasible in GRB blast waves. The large value of K_p means that the plasma is fully turbulent and has relativistic Alfvén speeds. Changes in $E_{max,syn}$ are only weakly dependent on the turbulence index q. By comparing the $q = 5/3$ and $q = 2$ results in equation (50), one finds that the parameter dependence typically varies $\propto 1/4$ power. Because the $q = 2$ result is much less complicated, we examine the $q = 2$ results for $p_{max,syn}$ from equation (50). When $\Gamma \gg 1$,

$$p_{max,syn} \cong 4.4 \times 10^{12} \frac{K_p}{e_b} (\frac{f_\Delta}{1/12})^{-1} (\frac{x_d}{x}) \frac{A^3}{Z^4} (\frac{\Gamma^2_{300}}{\mu^2 n_2^2 E_{54}})^{1/3} . \tag{51}$$

It is interesting to note that the standard parameters $\Gamma_{300} = E_{54} = n_2 = 1$ used here are the same as those found to give good spectral fits to gamma-ray bursts (Dermer et al. 2000), and these parameters also give protons with energies $\gg 10^{20}$ eV. An important difference between parameters is that $e_B \cong 10^{-4}$ in the spectral modeling, whereas here we let $e_B \cong 1$. The reason that e_B had to be so small in the spectral modeling was to avoid forming photon spectra resulting from cooling electron distributions, which are rarely observed in GRB spectra. But electrons will also be accelerated via gyroresonant stochastic particle processes. When particle acceleration is included, e_B can be much larger because acceleration competes with radiative losses and the formation of cooling electron distributions is avoided.

In stochastic acceleration of highly relativistic electrons, helicity effects and gyroresonance with different plasma waves are not so important as for lower energy electrons, so we can apply equation (51) to determine the peak of the synchrotron spectrum radiated by electrons. Synchrotron losses rather than the Hillas condition determines the maximum energy of electrons accelerated through stochastic gyroresonance acceleration with plasma turbulence. The observed peak frequency of the νF_ν spectrum from accelerated electrons in a GRB source at redshift z is given by

$$\nu_{max} \text{ (Hz)} = \frac{2.8 \times 10^6}{1+z} B\Gamma (\frac{p^e_{max}}{\Gamma})^2 \tag{52}$$

for $q = 2$, where p^e_{max} is $(m_p/m_e)^2$ smaller than $p_{max,syn}$ given by equation (51), and $A = Z = 1$. Thus

$$E_{pk} \text{ (keV)} = h\nu_{max} = \frac{75}{1+z} (\frac{x_d}{x})^2 (\frac{f_\Delta}{1/12})^{-2} \frac{K_p^2 \Gamma_{300}^{4/3}}{e_B^{3/2} \mu^{5/6} n_2^{5/6} E_{54}^{2/3}} \tag{53}$$

Equation (53) shows that E_{pk} is in the range of E_{pk} values observed with BATSE (Mallozzi et al. 1995) between $\approx$ 100 keV and 1 MeV when $\Gamma_0 \sim$ 300-3000. This effect may resolve a fine-tuning issue in the external shock scenario (Chiang and Dermer 1999) whereby the value of e_B has to be large enough to provide good radiative efficiency, but not so large that cooling electron distributions are formed.

4. Solutions to Particle Continuity Equation

We examine particle acceleration, escape, and losses within a GRB blast wave by employing a particle continuity equation

$$\frac{\partial N(p;t)}{\partial t} + \frac{\partial}{\partial p}[\dot{p}(p,t)N(p;t)] + \frac{N(p;t)}{t_{esc}(p,t)} = Q(p,t) . \tag{54}$$

The term $\dot{p}$ represents the total energy-change rate of particles due to acceleration, adiabatic and radiative processes, and t_{esc} is the particle escape timescale from the blast wave. Primes have been dropped to simplify the notation. The analytic solution to this equation when $\dot{p} = \dot{p}(p) < 0$ and $t_{esc} = t_{esc}(p)$ are independent of t is

$$N(p;t) = \frac{1}{|\dot{p}|} \int_p^\infty dp^* Q(p^*, t^*) \exp[- \int_p^{p*} \frac{dp''}{t_{esc}(p'')|\dot{p}(p'')|}] \tag{55}$$

where $t^* = t - \int_p^{p*} dp''/|\dot{p}(p'')|$. The solution for $\dot{p} > 0$ is obtained by reversing the limits on the integrals in the exponential and in the definition of t^*, and by integrating from 0 to p in the integration over p^*.

When the terms $\dot{p}$ and t_{esc} depend on both p and t, the solution to equation (54) can be obtained semi-analytically by inspection, giving

$$N(p;t) = \int_0^t dt_i \; Q[p_i(p,t,t_i),t_i] \; |\frac{dp_i}{dp}| \; \exp\{-\int_{t_i}^t \frac{dt^*}{t_{esc}[p_i(p,t,t^*),t^*]}\} \; , \tag{56}$$

where $p_i = p_i(p,t,t'')$ is obtained by inverting $p = p(p_i,t,t'')$, which solves $dp/dt = \dot{p}$. Equation (56) can be shown to reduce to equation (55) when t_{esc} and $\dot{p}$ are time-independent.

For particle acceleration in a blast wave, it is more convenient to consider the evolution of the comoving distribution function with location x. Using the relationship $dx = Pcdt'$ between radius and comoving time, equation (54) becomes

$$\frac{\partial N(p;x)}{\partial x} + \frac{\partial}{\partial p}\{[\frac{\dot{p}_m}{Pc} + (\frac{dp}{dx})_{adi}]N(p;x)\} + \frac{N(p;x)}{Pct_{esc}(p,x)} = Q(p,x) \; . \tag{57}$$

The term $\dot{p}_m$ represents the sum of the particle energy gain and loss rates, excluding adiabatic losses which are given through the term $(dp/dx)_{adi}$ from equation (12). Following equation (56), the solution to equation (57) is

$$N(p;x) = 4\pi n_0 \int_0^x dx_i \; C(x_i)x_i^2 \; \delta[p_i(p,x,x_i) - P(x_i)] \; |\frac{dp_i}{dp}| \; \exp\{-\int_{x_i}^x \frac{dx^*}{Pct_{esc}[p_i(p,x,x^*),x^*]}\} \; . \tag{58}$$

Here we substitute equation (15) for the source function Q, though modulated by the factor $C(x_i)$. Equation (58) can be solved analytically in some restricted cases, but must be solved numerically for the general case involving adiabatic losses and stochastic energy gains. When the energy lost through particle escape is a large fraction of the swept-up energy, the system departs from its adiabatic behavior. In this case, a more general numerical approach involving inversion of a tri-diagonal matrix must be used. We describe the numerical considerations for dealing with this system, though here we only report the results for blast waves that evolve in the adiabatic regime.

4.1. Analytic Solution

Equation (58) can only be solved analytically when the turbulence index $q = 2$. Depending on how the MHD turbulence develops and evolves, this case may be of primary interest. It is generally thought that wave energy is introduced on the largest length scales of the system and is transferred to smaller scales through nonlinear mode coupling (e.g., Zhou and Matthaeus 1990), to be dissipated through particle acceleration when the particle Larmor radii are in resonance with cascading turbulence. In the Kolmogorov phenomenology, the wave energy achieves a steady-state turbulence spectrum with index $q = 5/3$.

Particles can only be accelerated when $(dp/dx)_{sto} > |(dp/dx)_{adi}|$ (Section 3.2.2), that is, when $p \gtrsim (\Delta/r_{\rm L}^0)(f_\Delta/K_p)^{1/(q-2)}$ if $q > 2$, and when $p \lesssim (\Delta/r_{\rm L}^0)(f_\Delta/K_p)^{1/(2-q)}$ if $q < 2$. If $q > 2$, most of the MHD turbulence energy is contained in small wavevector (long wavelength) turbulence that accelerates high-energy particles with large Larmor radii, and vice versa for $q < 2$. Consequently, there will be a resonance gap that prevents particle acceleration when $q > 2$, because adiabatic losses dominate particle acceleration except for the very highest energy particles, of which there may be none if $(\Delta/r_{\rm L}^0)(f_\Delta/K_p)^{1/(q-2)} > P_0$. If the turbulence spectrum evolves to the Kolmogorov index through a progressive hardening of the turbulence spectrum, then the low-energy swept-up particles will begin to sample the evolving turbulence spectrum when $q = 2$. If $K_p \gtrsim f_\Delta$ and $q = 2$, stochastic acceleration will dominate adiabatic losses and accelerate particles to the highest energies. The waves will be damped by transferring their energy to the particles. In this way, a quasi-steady turbulence spectrum with $q \cong 2$ may be formed.

When $q = 2$ and $K_p \gtrsim f_\Delta$, the stochastic energy gain rate dominates the adiabatic energy-loss rate for all particle momenta. Thus $(dp/dx)_{sto} \cong K_p p/(P\Delta)$ from equation (41). In the limit $P \gg 1$, $(dp/dx)_{sto} \cong K_p p/(f_\Delta x)$ and, provided $K_t > 1$, $t_{esc} \cong K_t \Delta/c$ from equation (43). The particle momenta therefore evolve according to the relation $p = p_i(x/x_i)^{K_p/f_\Delta}$. Equation (58) becomes

$$N(p;x) = 4\pi n_0 \int_0^x dx_i \; C(x_i) x_i^2 \; \delta[p(\frac{x_i}{x})^{K_p/f_\Delta} - P(x_i)] \; (\frac{x}{x_i})^{-(K_p+1/K_t)/f_\Delta} \; . \tag{59}$$

There is no high-energy cutoff to the accelerated particle momentum in this limit, because the acceleration rate $(dp/dx)_{sto} \propto 1/x$ and thus rapidly accelerates particles at the earliest times.

When $x_i \ll x_d$, $P(x_i) \cong P_0$ and

$$N(p;x) = 4\pi n_0 \; C(\bar{x}_i) \; (\frac{f_\Delta x^3}{K_p P_0}) \; x^3 \; (\frac{P_0}{p})^{1+3f_\Delta/K_p+1/(K_p K_t)} \; , \tag{60}$$

where $\bar{x}_i = x(\frac{P_0}{p})^{f_\Delta/K_p}$. When $x_i \gg x_d$, $P(x_i) \cong P_0(x_i/x_d)^{-3/2}$ and

$$N(p;x) = \frac{4\pi n_0 \; C(\tilde{x}_i) \; \tilde{x}_i^2 \; (x/\tilde{x}_i)^{-(K_p+1/K_t)/f_\Delta}}{[K_p p(\tilde{x}_i/x)^{K_p/f_\Delta}/f_\Delta \tilde{x}_i] + [3P_0(\tilde{x}_i/x)^{-3/2}/2\tilde{x}_i]} \; , \tag{61}$$

where $\tilde{x}_i = \; (P_0 x_d^{3/2} x^{K_p/f_\Delta}/p)^{1/(K_p/f_\Delta+3/2)}$

Fig. 3 shows the comoving particle distribution function that results from stochastic gyroresonant acceleration by plasma turbulence with $q = 2$ and $K_p = 0.5$. We let $K_t = 2$ in Fig. 3a and $K_t = 10$ in Fig. 3b. The other parameters are the same as used in Figs. 1 and 2, namely $E_{54} = n_2 = \Gamma_{300} = e_B = 1$, and we let the modulation factor $C(x_i) = 1$. The particle distribution is multiplied by the factor $m_e c^2 p\gamma$ in order to indicate the energy contained in the accelerated particles. The comoving particle distribution is well-described by a power law spectrum, and the index depends sensitively on the assumed values of K_p and K_t. For these parameters, particles can reach ultra-high energies before the blast wave decelerates to nonrelativistic speeds, which occurs at $x \cong 45x_d$ for the chosen parameters. Because the escape timescale is independent of particle energy, power-law distributions of particles also escape from the blast wave. The highest energy escaping particles with large Larmor radii can freely escape to become UHECRs. In contrast, escaping particles with lower energies and smaller Larmor radii will be subject to the cosmic-ray adiabatic loss problem if their energy density exceeds the magnetic-field energy density in the local ISM.

4.2. Numerical Solution

To solve the continuity equation (58) numerically, we discretized this equation using a conservative finite differencing scheme. To this end we introduce

$$N_j^i = N(x_i, p_j) \; ; \;\; F_j^i = \dot{p}(x_i, p_j) N(x_i, p_j) \; . \tag{62}$$

Equation (58) becomes

$$\frac{N_j^{i+1} - N_j^i}{\Delta x} = \frac{F_{j+1/2}^{i+1} - F_{j-1/2}^{i+1}}{\Delta p} - \frac{N_j^{i+1}}{t_{esc}(x_i, p_j)} + Q_j^i \tag{63}$$

We make the identifications $N_j^{i+1} = N_i^j$ and $N_j^{i+1} = N_i^j$. This leads to larger diagonal elements in the resulting system of equations and enhances the stability of the numerical algorithm. As a result, we are led at each x-step to a tridiagonal system of equations for N_j^i, namely

$$a_j N_{j+1}^{i+1} + b_j N_j^{i+1} + c_j N_{j-1}^{i+1} = S_j^i \ , \tag{64}$$

where $a_j = 0$, $b_j = 1 + \Delta x[t_{esc}^{-1}(x_i, p_j) - \dot{p}/\Delta p]$, $c_j = \dot{p}\Delta x/\Delta p$, and $S_j^i = Q_j^i + N_j^i$. In our computations, the grid in p consisted of 10^4 intervals, with a linear spacing in the range $1 \leq p < 10^5$, and a logarithmic spacing in the range $10^5 \leq p < 10^9$. The step size in x $\Delta x = x_{j+1} - x_j$ was determined adaptively at each step to ensure that system (64) is well-behaved. The resulting Δx varied between 10^{10} and 10^{12} cm during the simulations.

Figs. 4 and 5 show the numerical simulation results for a Kolmogorov turbulence spectrum $q = 5/3$ when the blast wave reaches different locations between $0.1x_d$ and $10x_d$. The evolution of the blast wave is assumed to follow the adiabatic behavior described by equation (29). We use $K_p = 0.1$, and $K_t = 10$ in Fig. 4, and $K_p = 1$ and $K_t = 10$ in Fig. 5. The other parameters are the same as used in Fig. 4. Panel (a) in the figures show the time evolution of the comoving particle distribution, and panel (b) shows the cumulative energy distribution function of escaping particles measured by an outside observer, obtained by solving

$$N_{esc}(p_{esc}; x) = \int_0^\infty d\bar{x} \ \frac{N_{esc}[p_{esc}/\Gamma(\bar{x}), \bar{x}]}{\Gamma(\bar{x})} \ , \tag{65}$$

where $N_{esc}(p, x) = N(p; x)/Pct_{esc}(p, x)$ from equation (57).

In Fig. 4, we let the modulation factor $C(x_i) = 1$. The development of the internal comoving particle distribution is shown in Fig. 4a at different blast-wave locations. The particles diffuse to higher energies with time, reaching a maximum value that is about an order-of-magnitude less than the maximum momentum permitted through the available-time constraint that was estimated from equation (44). This expression does not, however, take into account adiabatic losses which appreciably retard acceleration of the highest energy particles. Fig. 4b shows the escaping particle distribution that would be measured in an external system. Most of the energy is carried by the very highest energy particles with energies between 10^{18} and 10^{20} eV.

The escaping UHECRs carry more than 10^{56} ergs of energy, because wave damping and energy conservation have not been taken into account in the calculation. A realistic calculation must consider these processes, as in treatments of impulsive Solar flares (e.g., Miller 1998; Miller and Roberts 1995). Moreover, we have restricted the blast wave evolution to the adiabatic regime. The calculation of Fig. 4 does not violate energy conservation or the assumption of an adiabatic blast wave if we assume that $C(x_i) \lesssim 10^{-3}$, so that only a very small fraction of swept-up particles are accelerated to the highest energies. It is artificial to assume that $C(x_i)$ does not change with time location, but a self-consistent treatment of wave cascading and damping, required to obtain a correct evaluation of $C(x_i)$, is beyond the scope of this paper.

In Fig. 5 we show a calculation of the evolving particle distribution with $K_p = 1$. Here we assume that $C(x_i) = 10^{-4}$ so that the calculation is self-consistent. The effect of increasing the rate constant K_p is to permit particle acceleration to much higher energies, until adiabatic losses and escape suppress further acceleration. Fig. 4b shows that a significant fraction of the energy is carried by particles with energies $\gtrsim 10^{20}$ eV. In this calculation, the cumulative escaping particle spectrum develops a spectrum with number index ~ -3. Larger values of K_t or other parameters of the calculation, such as Γ_0, can yield even higher energy escaping particles. Thus stochastic particle acceleration in relativistic blast waves can, in principle, produce cosmic rays with energies $\gtrsim 10^{20}$ eV.

4.3. Cosmic Ray and Ultra-High Energy Cosmic Ray Origin

As shown in Figs. 4 and 5, protons accelerated to $\gtrsim 10^{19}$ eV by a Kolmogorov MHD turbulence spectrum can diffusively escape from the blast wave during the prompt and afterglow phases of a GRB to become UHECRs. The Larmor radii of these particles is so large that they do not strongly couple with the interstellar gas and thereby avoid further adiabatic losses. This is because the energy density of UHECRs within a volume defined by their Larmor radius is smaller than the energy density of the mean magnetic field within that volume. UHECRs consequently behave as isolated particles rather than as a relativistic fluid that does work on its surroundings.

This is not the case for lower energy particles which, if they escaped into the ISM, would generate streaming instabilities that would strongly couple these particles with the ISM. The adiabatic loss problem would be severe for these particles. As shown by the simulations, however, only the very highest energy particles escape during the relativistic phases of the blast wave. Once the blast wave enters the nonrelativistic Sedov phase, stochastic acceleration to ultra-high energies is no longer possible because the Alfvén speed becomes $\ll c$. During this phase, shock Fermi acceleration becomes more efficient than stochastic acceleration. The internal particle population confined by the blast wave loses energy due to adiabatic expansion of the blast wave shell, but also begins to be energized through shock acceleration. The nonrelativistic phase of a GRB remnant evolution resembles a very energetic SNR, though differing from a conventional SNR by containing a population of high energy particles available from the earlier acceleration episode. Consequently the timescale constraint (Lagage and Cesarsky 1983) on shock Fermi acceleration is relaxed. Cosmic rays will leave the remnant as the SNR dissipates in the ISM so that the cosmic-ray adiabatic loss problem is solved, as in the standard model, by shock acceleration taking place throughout the expansion of the SNR until the energy density of the relativistic particle fluid is small compared to the magnetic-field energy density of the ISM.

Future work must treat both first- and second-order particle acceleration in a relativistic blast wave that decelerates to nonrelativistic speeds and determine whether this scenario can satisfactorily explain the origin of the hadronic cosmic rays.

5. Summary and Conclusions

As described in the Introduction and elsewhere (Dermer 2000), there are severe observational and theoretical difficulties in the supernova hypothesis for the origin of the cosmic rays. Only two classes of Galactic sources have power comparable to that produced by SNe, namely stellar winds and high-mass stars that collapse to black holes while making GRBs (Dermer 2000a). Stellar winds are not feasible for efficient CR acceleration because the wind speeds, $\lesssim 3000$ km s^{-1}, imply an unacceptably large acceleration timescale. Even for supernova shocks with shock speeds reaching $\sim 10^4$ km s^{-1}, acceleration to energies near the knee of the CR spectrum is only marginally possible. SNR particle acceleration to energies above the knee of the cosmic ray spectrum depends critically on an assumed distribution of shock obliquities, the dependence of acceleration efficiency on shock obliquity, and spatial limitations (Ellison et al. 1995; Baring et al. 1999), all of which are poorly known.

Because the Alfvén speed approaches c whenever the magnetic field approaches its equipartition value in relativistic shocks, second-order Fermi acceleration can be much more efficient than first-order Fermi acceleration in GRB blast waves. In nonrelativistic SNR shock waves, by contrast, the first-order process dominates. Consequently, we have considered particle acceleration through stochastic gyroresonant acceleration in GRB blast waves during their relativistic phases. Even in the highly simplified approach developed here, it was necessary to treat adiabatic losses correctly in the expanding blast wave. This was dealt with in Section 2, where an equation for blast-wave evolution was derived (equation (5)) that contains a term that rechannels the energy lost by adiabatic expansion of the nonthermal particles into the directed outflow of the blast wave. An expression for the energy lost through adiabatic expansion by a general particle distribution function that contains both relativistic and nonrelativistic particles was derived in Section 2.2. The evolution of the internal particle distribution due to adiabatic losses was treated in Section 2.3, and an expression describing the evolution of an adiabatic blast wave , in agreement with numerical calculations, was shown to reduce to well-known results in the nonrelativistic regime in Section 2.4.

In Section 3 we showed that ultra-high energy particle production in GRB blast waves satisfies the Hillas condition, which compares the particle Larmor radius with the size scale of the system. In the case of the GRB system, the size scale is the blast-wave width. Thus GRBs are allowed sites for UHECR production. We employed simplified forms for the energy gain rate and escape time scale due to stochastic gyroresonant interactions of particles with MHD turbulence, based upon expressions derived in the quasilinear approximation. In Section 3.2, we derived the conditions under which competition between stochastic acceleration, available time, adiabatic losses, and diffusive escape permits acceleration to ultra-high energies. The conditions under which synchrotron losses limit particle acceleration were also examined. We find that wide ranges of parameter values permit particle acceleration to ultra-high energies through stochastic gyroresonant processes in GRB blast waves. In Section 4, we numerically calculated comoving and escaping particle distributions by employing a continuity equation, and found that a population of UHECRs will diffusively escape from GRB blast waves during the prompt and afterglow phases.

This study is preliminary and does not address the question of the origin of the turbulence, nor wave cascading and damping. Within the constraints of the problem that are rather well defined, for example, the maximum blast-wave magnetic field, the characteristic blast-wave width, the adiabatic loss rate, and the time available for acceleration, we conclude that particle acceleration to ultra-high energies is possible in GRB blast waves. This process therefore offers a new approach to UHECR acceleration, and may also shed light on the unsolved problem of the origin of the hadronic cosmic rays.

We thank A. Achterberg, M. Baring, L. O'C. Drury, A. Levinson, J. A. Miller, and H. Völk for discussions. The work of C.D. is supported by the Office of Naval Research and the NASA Astrophysics Theory Program (DPR S-13756G).

REFERENCES

Allen, G. E., et al. 1997, ApJ, 487, L97

Barbosa, D. D. 1979, ApJ, 233, 383

Baring, M. G., Ellison, D. C., Reynolds, S. P., Grenier, I. A., and Goret, P. 1999, ApJ, 513, 311

Blandford, R. D., and Eichler, D. 1987, Phys. Rep., 154, 1

Blandford, R. D., and McKee, C. F. 1976, Phys. Fluids, 19, 1130

Bloemen, J. B. G. M., Blitz, L., and Hermsen, W. 1984, A&A, 279, 136

Böttcher, M., and Dermer, C. D. 2000, ApJ, 532, 281

Bogdan, T. J., Lee, M. A., and Schneider, P. 1991, JGR, 96, 161

Buckley, J. H., et al. 1998, A&A, 329, 639

Chevalier, R. A. 1974, ApJ, 188, 501

Chiang, J., and Dermer, C. D. 1999, ApJ, 512, 699

Cowsik, R., and Wilson, L. W. 1975, Proc. 14th ICRC, Munich, 2, 475

Dermer, C. D., and Chiang, J. 1998, New Astronomy, 3, 157

Dermer, C. D. 2000, ApJ, submitted (astro-ph/0005440)

Dermer, C. D. 2000a, in Heidelberg 2000 Gamma Ray Workshop, ed. F. A. Aharonian and H. Völk (AIP: New York), in press (astro-ph/0010564)

Dermer, C. D., and Böttcher, M. 2000, ApJ, 534, L155

Dermer, C. D., Chiang, J. and Mitman, K. E. 2000, ApJ, 537, 785

Dermer, C. D., Chiang, J. and Böttcher, M. 1999, ApJ, 513, 656

Dermer, C. D., Miller, J. A., and Li, H. 1996, ApJ, 456, 106

Drury, L. O'C. 1983, Rep. Prog. Phys., 46, 973

Ellison, D. C., Baring, M. G., and Jones, F. C. 1995, ApJ, 453, 873

Esposito, J. A., Hunter, S. D., Kanbach, G., and Sreekumar, P. 1996, ApJ, 461, 820

Falle, S. A. E. G. 1981, MNRAS, 195, 1011

Gaisser, T. K. 1990, Cosmic Rays and Particle Physics (New York: Cambridge University Press), 148

Gallant, Y. A., and Achterberg, A., 1999, MNRAS, 305, L6

Ginzburg, V. L., and Syrovatskii, S. I. 1964, The Origin of Cosmic Rays (New York: MacMillan)

Hayakawa, S. 1969, Cosmic Ray Physics (New York: Wiley-Interscience)

Hillas, A. M. 1984, ARAA, 22, 425

Huang, Y. F., Dai, Z. G., and Lu, T. 1999, Chinese Phys. Lett., 16, 775

Huang, Y. F., Dai, Z. G., and Lu, T. 1999, MNRAS, 309, 513

Hunter, S. D., et al. 1997, ApJ, 481, 205

Keohane, J. W., et al. 1997, ApJ, 454, 350

Koyama, K., Petre, R., Gotthelf, E. V., Hwang, U., Matsuura, M., Ozaki, M., and Holt, S. S. 1995, Nature, 378, 255

Lagage, P. O., and Cesarsky, C. J. 1983, A&A, 118, 223

Lozinskaya, T. A. 1992, Supernovae and Stellar Wind in the Interstellar Medium (New York: AIP)

Mallozzi, R. S., et al. 1995, ApJ, 454, 597

Melrose, D. B. 1974, Solar Phys., 37,353

Mészáros, P., and Rees, M. J. 1993, ApJ, 405, 278

Miller, J. A. 1998, Space Sci. Rev., 86, 79

Miller, J. A., and Roberts, D. A. 1995, ApJ, 452, 912

Miller, J. A., and Ramaty, R. 1989, ApJ, 344, 973

Moderski, R., Sikora, M., and Bulik, T. 2000, ApJ, 529, 151

Nagano, M., and Watson, A.A. 2000, RMP, 72, 689

Norman, C. A., Melrose, D. B., and Achterberg, A. 1995, ApJ, 454, 60

Panaitescu, A., Mészáros, P., and Rees, M. J. 1998, ApJ, 503, 314

Piran, T. 1999, Phys. Reports, 314, 575

Pohl, M., and Esposito, J. A. 1999, ApJ, 507, 32

Pohl, M., and Schlickeiser, R. 2000, A&A, 354, 395

Protheroe, R. J., and Szabo, A. P. 1992, Phys. Rev. Lett., 69, 2885

Schlickeiser, R. 1989, ApJ, 336, 243

Schlickeiser, R., and Dermer, C. D. 2000, A&A, 360, 789

Sari, R., Narayan, R., and Piran, T. 1996, 473, 204

Simpson, J. A. 1983, Annual Review of Nuclear and Particle Physics, 33, 323

Steinacker, J., and Miller, J. A. 1992, ApJ, 393, 764

Sturner, S. J., Skibo, J. G., Dermer, C. D., and Mattox, J. R. 1997, ApJ, 490, 619

van Paradijs, J., Kouveliotou, C., and Wijers, R. A. M. J. 2000, ARA&A, in press

Vietri, M. 1995, ApJ, 453, 883

Waxman, E. 1995, Phys. Rev. Lett., 75, 386

Waxman, E., and Bahcall, J. N. 2000, ApJ, 541, 707

Zhou, Y., and Matthaeus, W. H. 1990, JGR, 95, 14881

This preprint was prepared with the AAS LaTeX macros v5.0.

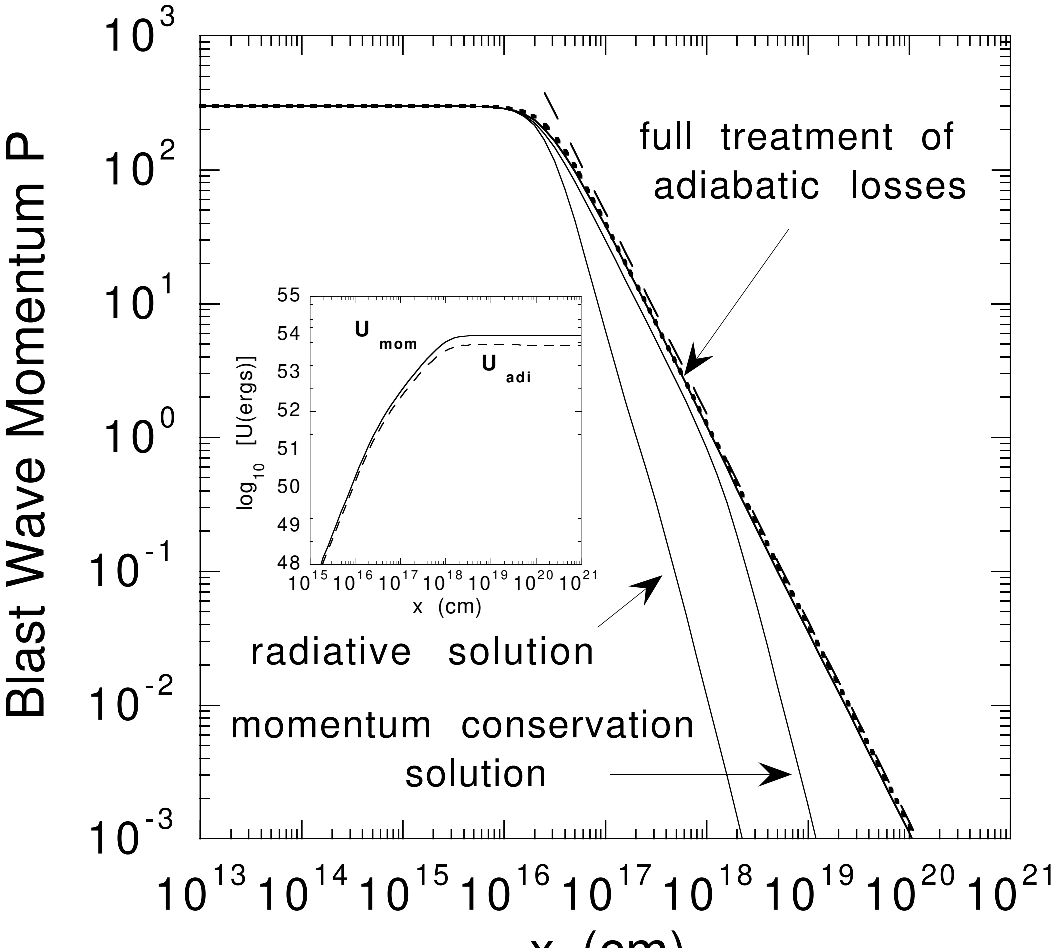

Fig. 1.— Evolution of blast wave momentum P for different assumptions for the particle energy losses. The solid curve labeled "full treatment of adiabatic losses" is a numerical solution of equation (5) that includes adiabatic losses of swept-up particle energy that is transformed into the directed kinetic energy of the outflow. The curve labeled "momentum conservation solution" neglects adiabatic energy losses of the swept-up particles, and the curve labeled "radiative solution" assumes that the internal energy is promptly radiated. Solid lines are hydrodynamic approximations at relativistic and nonrelativistic momenta, and the dotted curve is equation (29). The inset shows the evolution of the internal energy U_{mom} and U_{adi} for the momentum-conservation and adiabatic solutions, respectively.

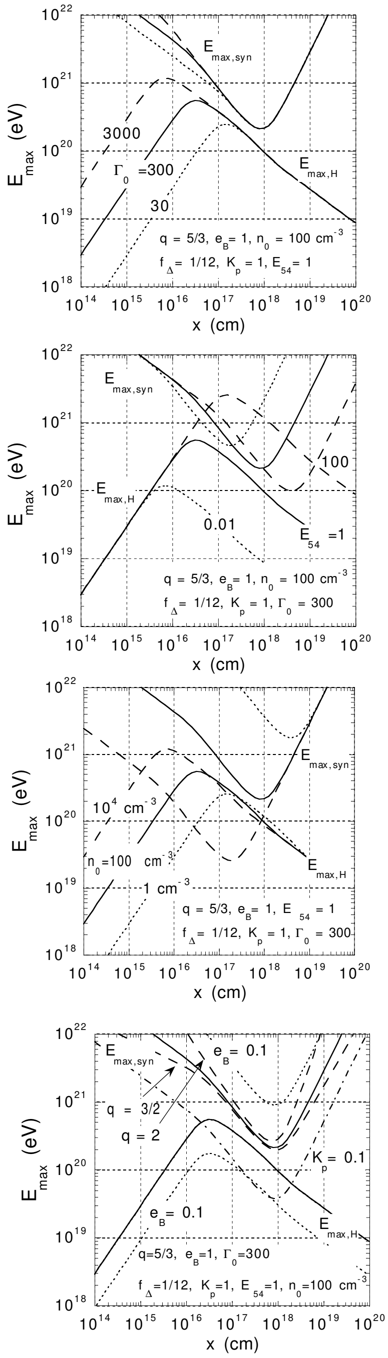

Fig. 2.— Maximum proton energies E_{max} as a function of blast wave location x implied by the Hillas condition, equation (34), obtained by comparing the Larmor radius and blast wave width, and $E_{max,syn}$ from equation (50), obtained by comparing the stochastic acceleration rate with the synchrotron cooling rate. Standard parameters are shown in the figure legend. Changes in E_{max} and $E_{max,syn}$ for different values of Γ_0, E_{54}, and n_0 are shown in (a), (b), and (c), respectively. Changes in $E_{max,syn}$ for different turbulence spectral indices q and acceleration rates K_p, and e_B are shown in (d), as well as changes in E_{max} and $E_{max,syn}$ due to changing e_B values.

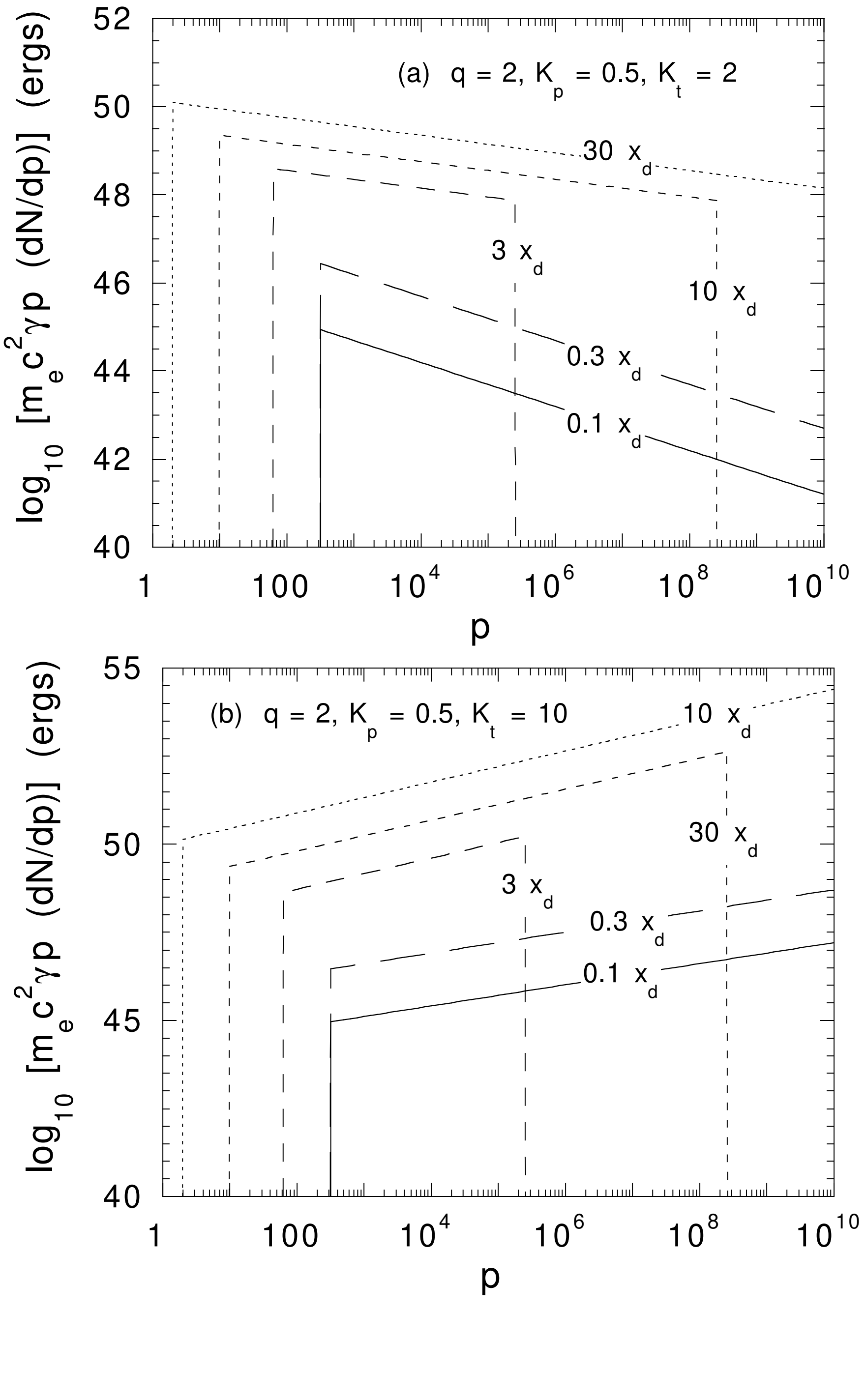

Fig. 3.— Evolution of comoving particle distribution at different locations x of the blast wave in units of the deceleration radius x_d for the analytic result, equations (60) and (60), for a turbulence spectrum with $q = 2$. Parameters are $E_{54} = 1$, $n_0 = 100$ cm^{-3}, $\Gamma_0 = 300$, and $f_\Delta = 1/12$. In panel (a), $K_p = 0.5$ and $K_t = 2$. In panel (b), $K_p = 0.5$ and $K_t = 10$.

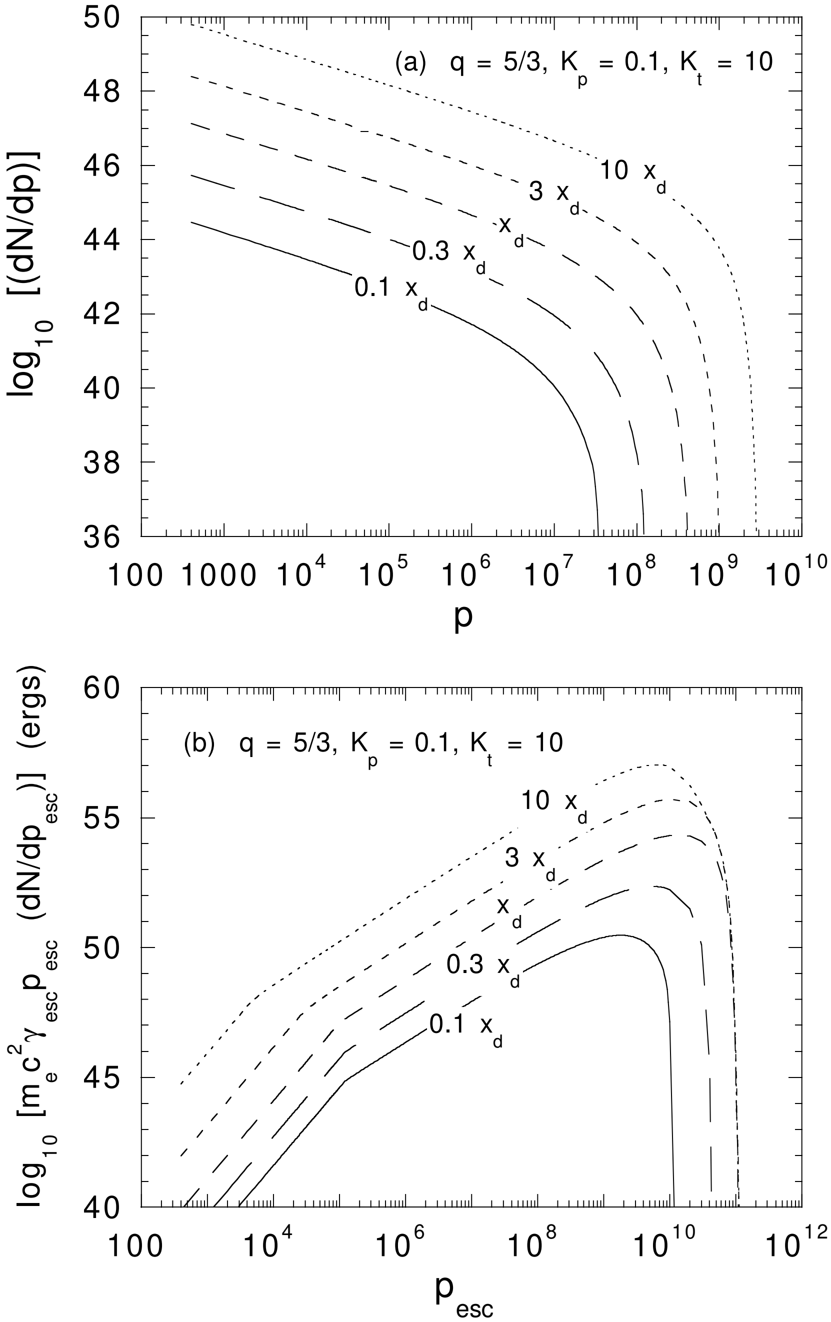

Fig. 4.— Numerical calculation of the comoving particle distribution in panel (a), and the escaping particle distribution in panel (b) at different blast-wave locations. Parameters are the same as in Fig. 3, except that $q = 5/3$, $K_p = 0.1$ and $K_t = 10$.

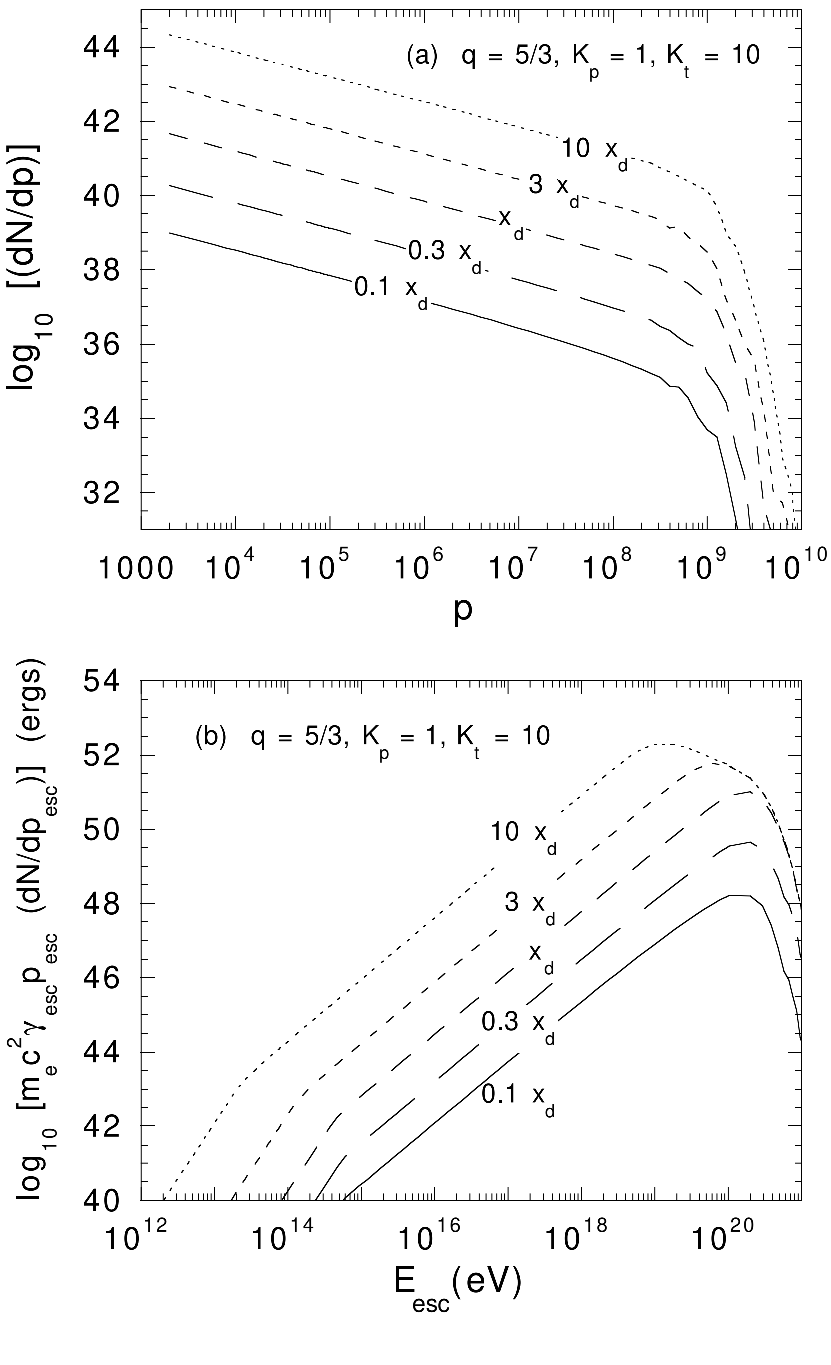

Fig. 5.— Same as Fig. 4, except that $K_p = 1$ and $K_t = 10$.